

An Analog Cellular Automaton Model of Maxwell-Dirac Electrodynamics

Randall C. O'Reilly

*University of Colorado Boulder
345 UCB
Boulder, CO 80309
Randy.OReilly@colorado.edu*

Submitted to Physical Review A, March 15, 2006

(Dated: March 15, 2006)

The coupled Maxwell-Dirac electrodynamic system is implemented in an analog (continuous-valued) cellular-automaton operating within a three dimensional regular face-centered cubic lattice. This system consists of a second-order Dirac wave equation for the electron (i.e., the minimally-coupled Klein-Gordon equation with spin, operating on two complex state variables), coupled with electromagnetic potential field versions of Maxwell's equations in the Lorenz gauge. Both Dirac and Maxwell's equations are standard second-order wave equations with some additional terms. An analog cellular automaton produces such wave equations as one of the simplest possible models that exhibits any physically interesting behavior. Furthermore, it avoids standard objections by achieving rotationally symmetric propagation at cellular-scales through the use of a 26 neighbor update equation for the laplacian. To achieve numerical stability, parity must be broken, which may provide an explanation for properties of the weak force. The behavior of an electron trapped by a fixed positive charge is simulated, providing a model of the hydrogen atom system. Overall, this framework may provide an appealing mechanistic model of electrodynamics.

I. INTRODUCTION

This paper presents an analog (continuous-valued) cellular automaton (CA) model [1, 2] of the coupled Maxwell and Dirac equations, as in the neoclassical or semiclassical approach to quantum electrodynamics [3–9]. Neoclassical quantum electrodynamics uses the Schrödinger or Dirac equation for an electron, self-coupled with Maxwell's electromagnetic field equations, as an alternative to standard quantum electrodynamics (QED). The self-coupling of the electron with its own electromagnetic field results in nonlinear interactions that, while difficult to analyze, appear to give rise to the phenomena described in terms of virtual particle dynamics in standard QED. The present system consists of the second-order Dirac equation (i.e., the minimally-coupled Klein-Gordon equation with spin, operating on two complex field variables), coupled with Maxwell's equations for electromagnetic potentials in the Lorenz gauge.

The primary result of this paper is to show that the neoclassical picture emerges naturally from an attempt to construct the simplest possible CA model that is consistent with known electrodynamics. Both the Dirac and Maxwell equations in this system are standard second-order wave equations, with additional terms. The second-order wave equation can be seen as one of the simplest possible analog CA models that does anything interesting at all. Thus, this model represents a very simple, computationally explicit framework for quantum electrodynamics.

CA models have been dismissed in the past because of their lack of rotational symmetry caused by the underlying cubic lattice. The present model does not suffer from this problem. Specifically, by using continuous-valued state variables in a regular cubic lattice with a full 26 neighbor stencil, interacting via second-order wave equations, rotational asymmetry in propagation is almost completely eliminated. It is only present at small levels in extremely high frequency waves (i.e., close to grid scale). Given that the lattice cubes are at the Planck length scale ($1.6162 \times 10^{-33} \text{ cm}$), such effects would almost certainly be unobservable in any real experiment. In contrast, previous quantum CA models have used smaller

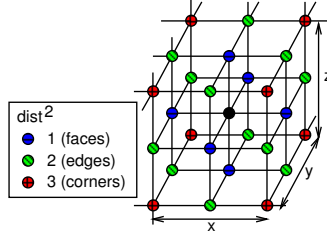


Figure 1: Face-centered cubic tiling of space, showing centers of cells as nodes, with all 26 neighbors of a given cell shown. This is the neighborhood over which cells interact. The squared distances of the neighbors (shown) weight their contributions.

neighborhood stencils and first-order equations, which typically do not produce rotationally symmetric propagation at any scale.

To demonstrate its basic properties, the CA system was simulated on a small scale, where it can produce a stable hydrogen atom model in terms of an electron charge distribution tapped by a fixed central positive charge representing the nucleus. To make the system numerically stable, parity must be broken in the ordering of wave variable updates. This parity breaking is intriguing given the similar kind of parity breaking present in the weak force.

The paper is organized as follows. First, the analog CA framework is developed, showing how the standard second-order wave equation emerges as one of the simplest possible set of update equations that do anything interesting at all. Then, the Maxwell and Dirac equations are developed within this framework. The hydrogen atom model is then described, followed by a discussion of various unresolved issues.

II. CONTINUOUS CA FRAMEWORK AND THE WAVE EQUATION

CA models are appealing because they represent arguably the simplest way of implementing physical processes: space is carved into a lattice of identical small cubes (cells), each cell contains one or more state variables, and physics emerges through the local interactions between these cells (Figure 1). A number of different CA models of various physical and other phenomena have been developed, and their potential virtues as physical models discussed [1, 2, 10–14]. Most of these CA models involve discrete (binary) state variables (i.e., a *digital* CA), and despite all the promising efforts, nobody has yet come up with a binary-state CA system that produces something like quantum electrodynamics. However, by introducing continuous-valued state variables (i.e., an *analog* CA), several researchers have been able to model the evolution of fundamental quantum wave functions [1, 2]. The present model also adopts continuous-valued state variables.

The introduction of continuous-valued states would seem to be a significant departure from the minimalist philosophy that motivates the use of CA models in the first place. From a the perspective of implementing the system on a digital computer, a single binary state is the simplest, most fundamental entity, and continuous values are only available in approximate form via floating point numbers, which are composed of binary states. However, the notion of the universe as a digital computer might not be the best model: perhaps it is instead a kind of analog computer, where continuous-valued analog states are a primitive of the system, instead of discrete states? Furthermore, there is another component of the overall simplicity of the system that is often ignored: the simplicity of the CA update equations. In virtually all binary-state CA's, the update equations need to be asymmetric, non-monotonic, and overall quite complex to achieve interesting behaviors. In contrast, with continuous-valued state variables it is possible to have very interesting physical behavior emerge by computing a simple average of the local neighborhood state values. Thus, one might plausibly argue that the functional simplicity of analog CA's outweighs any perceived cost associated with introducing continuous-valued states. Furthermore, continuous-valued states are critical for eliminating the

rotational asymmetry problem, as mentioned earlier. In any case, the bottom line is that we can produce an accurate simulation of quantum electrodynamics using an analog CA, as described below.

To develop the analog CA model, it is instructive to enumerate a sequence of CA update equations, starting with the simplest possible case, and working toward one that exhibits some potentially interesting physical behavior. Our starting point is to set the new state of each cell equal to the average of the neighbor's states, which is arguably one of the simplest possible neighborhood interactions in a continuous-valued system:

$$s_i^{t+1} = \frac{1}{26} \sum_{j \in \mathcal{N}_i} s_j^t. \quad (1)$$

Each cell's state is represented by s_i^t , indexed spatially by subscript $i = (x_i, y_i, z_i)$ and temporally by superscript t , and the neighborhood \mathcal{N} indicates the 26 adjacent neighbors of each cell, as shown in Figure 1. This system does not produce any interesting physical behavior: it just converges to an equilibrium average state. A reasonable next step in complexity would be to operate on the difference between the neighbor average value and the current state value, so that the system is driven by the “tension” or “stress” across the states:

$$s_i^{t+1} = \frac{1}{26} \sum_{j \in \mathcal{N}_i} s_j^t - s_i^t. \quad (2)$$

This produces the opposite behavior: divergence to infinity for any non-uniform initial starting state. Using this difference term as an update increment to the existing state value is the same as equation 1.

As a next step up in complexity, a rate of change of the state \dot{s} (i.e., a velocity) can be introduced, which can be set to the neighborhood difference term:

$$\dot{s}_i^{t+1} = \dot{s}_i^t + (g(\mathcal{N}_i^t) - s_i^t), \quad (3)$$

with the overall state variable updated accordingly:

$$s_i^{t+1} = s_i^t + \dot{s}_i^{t+1}. \quad (4)$$

At this point, we cross a critical threshold, and the system produces physically interesting wave dynamics. Indeed, this is essentially the standard second-order wave equation, modulo proper neighborhood weighting terms as shown below.

One can conclude from this exercise that the second-order wave equation is arguably one of the simplest possible continuous-valued CA update equations that does anything physically interesting. We show below that all of electrodynamics can be built out of elaborations of this one fundamental interaction. This seems like a compelling argument in favor of the idea that this kind of analog CA model provides a particularly simple, elegant way of modeling fundamental physics.

A. Formalization of the 26-Neighbor Discrete Laplacian Approximation

In continuous space-time coordinates, the wave equation is typically expressed in terms of the laplacian $\nabla^2 = \left(\frac{\partial^2}{\partial x^2} + \frac{\partial^2}{\partial y^2} + \frac{\partial^2}{\partial z^2} \right)$:

$$\frac{\partial^2 s}{\partial t^2} = c^2 \nabla^2 s, \quad (5)$$

where c is the speed of light, which is 1 in the Planck scale units that are the natural units for this system. In [15], we show that the laplacian can be accurately approximated by using a stencil that includes all 26 neighbors:

$$\nabla^2 s_i \approx \nabla_{26}^2 s_i \equiv \frac{3}{13} \sum_{j \in \mathcal{N}_{26}} k_j (s_j - s_i), \quad (6)$$

where k_j is a factor that weights the different neighbors differentially according to their distance from the central cell:

$$k_j = \frac{1}{d^2}, \quad (7)$$

and d is the Euclidean distance to the neighbor j :

$$\begin{aligned} \text{faces: } k_j &= 1 \\ \text{edges: } k_j &= \frac{1}{2} \\ \text{corners: } k_j &= \frac{1}{3}. \end{aligned} \quad (8)$$

In the discrete space-time of our CA model, this implies the following update equations, using \ddot{s} to represent the second temporal derivative of the state value:

$$\ddot{s}_i^{t+1} = c^2 \nabla_{26}^2 s_i^t = c^2 \frac{3}{13} \sum_{j \in \mathcal{N}_{26}} k_j (s_j^t - s_i^t), \quad (9)$$

$$\dot{s}_i^{t+1} = \dot{s}_i^t + \ddot{s}_i^{t+1}, \quad (10)$$

$$s_i^{t+1} = s_i^t + \dot{s}_i^{t+1}. \quad (11)$$

As we show in [15], this approximation exhibits a very high degree of spatial symmetry, such that waves propagate outward from a given point in all directions at the same speed, with the same magnitude, etc. Only at the highest frequencies, at the scale of the underlying grid, are there measurable deviations from symmetry, and these remain small. This high degree of symmetry is due to the use of all 26 neighbors in the computation. Furthermore, it depends critically on the second-order nature of the wave equation. Other first-order versions of wave equations do not exhibit such natural symmetry in three dimensions [1].

III. MAXWELL'S EQUATIONS IN POTENTIAL FORM IN THE LORENZ GAUGE

It is well known (e.g., [16]) that Maxwell's equations can be expressed in terms of standard wave equations operating on the scalar potential A_0 and the vector potential $\vec{A} = (A_x, A_y, A_z)$:

$$\frac{\partial^2 A_0}{\partial t^2} = c^2 \nabla^2 A_0 + \frac{1}{\epsilon_0} \rho, \quad (12)$$

$$\frac{\partial^2 \vec{A}}{\partial t^2} = c^2 \nabla^2 \vec{A} + \mu_0 \vec{J}, \quad (13)$$

where ρ is the charge density and \vec{J} is the charge current density. In our analog CA model, Maxwell's equations can therefore be represented by four update equations, one for each variable, all of the form of

the standard wave equation plus an additional “source” driving term (charge or current). For the scalar potential, we have:

$$\ddot{A}_{0i}{}^{t+1} = c^2 \nabla_{26}^2 A_{0i}{}^t + \frac{1}{\epsilon_0} \rho^t. \quad (14)$$

For the vector potential, there are three equations of this form, one for each of the three dimensions (x, y, z) of the vector. For example, the equations for the x dimension are:

$$\ddot{A}_{xi}{}^{t+1} = c^2 \nabla_{26}^2 A_{xi}{}^t + \mu_0 J_x^t. \quad (15)$$

The measurable electric (\vec{E}) and magnetic (\vec{B}) vector fields can be computed from these potentials as follows:

$$\vec{E} = -\vec{\nabla} A_0 - \frac{\partial \vec{A}}{\partial t}, \quad (16)$$

$$\vec{B} = \vec{\nabla} \times \vec{A}. \quad (17)$$

These enter into the coupling with the electron charge field as described later.

The simple wave form of Maxwell's equations requires that the Lorenz condition be satisfied:

$$\frac{\partial A_0}{\partial t} = -c^2 \vec{\nabla} \cdot \vec{A}. \quad (18)$$

Nothing is explicitly done in the system to enforce this condition, but the simulation results reported later show that the system automatically satisfies it to an error level of around 1×10^{-4} , with the error continuing to drop over time. Furthermore, this Lorenz error appears to be a function of the scale of frequencies of waves in the system relative to the grid scale: at realistic frequencies many orders of magnitude larger than the grid scale, this error would be entirely negligible.

In short, in this model, the electromagnetic field is a wave field propagating over four state variables through space, with the local charge and current state values (to be defined next) providing a driving force. The simplicity and elegance of this model are compelling, especially in light of the idea that the wave function is one of the simplest possible CA functions that does anything physically useful. It should also be noted that these equations are manifestly covariant, and thus embody all of the relevant properties of special relativity. Thus, a very large swath of fundamental physics can be accounted for using a very simple framework.

IV. THE SECOND-ORDER DIRAC EQUATION FOR AN ELECTRON

To model the electron, we use the second-order version of the Dirac equation [17, 18]. In standard quantum theory, the first-order Dirac equation can be used to describe the evolution of the quantum probability density function for an electron, even at relativistic energies (unlike the nonrelativistic Schrödinger's equation). The second-order version uses two complex state variables instead of the four needed for the first-order version, but otherwise describes the same underlying physics (in effect, the first derivatives in the second order equation represent an independent degree of freedom that is otherwise represented by the additional state variables in the first-order version). It is well known that the Dirac equation has some puzzling characteristics in the standard probabilistic framework of quantum physics. For example, it produces both positive and negative “probability” values. The negative “probability” values are interpreted as the probabilities of the electron antiparticle, the positron. An alternative interpretation that was pursued initially by Schrödinger in 1926, and has been pursued more recently in neoclassical self-coupled field theory

[3–9], is that the Dirac equation describes a conserved field of charge value, with the electron and positron having opposite charges. This interpretation is also adopted without much further comment in some modern textbooks [19–21].

It is instructive to progressively derive the second-order Dirac equation from the simpler Klein-Gordon (KG) equation [22–24], which is in turn a simple extension of the standard wave equation. The following derivation, except for the final step of the second-order Dirac equation, is based on [19, 20]. In the standard wave equation, waves always propagate at the same speed (c), which is appropriate for electromagnetism, but not for massive particles. The KG equation adds one simple mass term that allows waves to travel at a range of different speeds:

$$\frac{\partial^2 \varphi}{\partial t^2} = c^2 \left(\nabla^2 - \frac{m_0^2 c^2}{\hbar^2} \right) \varphi, \quad (19)$$

where we use φ to refer to a scalar charge-field state variable, and m_0 is the rest mass of the electron. The speed of wave propagation depends on the relationship between the overall “curvature” of the wave ($\nabla^2 \varphi$) and the squared-mass value $m_0^2 \varphi$. Intuitively, the mass slows the wave propagation force represented by $\nabla^2 \varphi$. Therefore, for the wave to move faster, a higher frequency wave (with larger $\nabla^2 \varphi$ values) is required. Thus, this equation captures the fundamental momentum-frequency relationship of quantum theory: $p = \frac{\hbar}{c} f$.

More formally, the KG equation can be derived from the relativistic energy-momentum equation, showing that the KG equation describes the propagation of a “particle” (as a wave of charge) that obeys conservation of energy, and special relativity (and Newtonian mechanics in the limit of slow velocities relative to the speed of light). The relativistic Hamiltonian (total energy) of the system, is:

$$E^2 = \vec{p}^2 c^2 + (m_0 c^2)^2, \quad (20)$$

which can be turned into a wave equation through the following standard operator definitions for energy E and momentum p :

$$E = i\hbar \frac{\partial \varphi}{\partial t}, \quad (21)$$

$$\vec{p} = i\hbar \vec{\nabla} \varphi, \quad (22)$$

where $\vec{\nabla} = \left(\frac{\partial}{\partial x}, \frac{\partial}{\partial y}, \frac{\partial}{\partial z} \right)$. Substituting the above operator definitions in place of the E and p terms, we recover the basic KG equation:

$$\frac{\partial^2 \varphi}{\partial t^2} = c^2 \left(\nabla^2 - \frac{m_0^2 c^2}{\hbar^2} \right) \varphi. \quad (23)$$

In short, this simple equation captures the major dynamical properties of particle motion. The fact that it is such a simple modification to the standard wave equation, which again is one of the simplest possible CA equations, provides a compellingly simple physical picture.

A. Charge and Complex Fields

The scalar KG equation does not produce a conserved charge value. However, the same basic equation operating on a complex field variable ($\phi = \varphi_a + i\varphi_b$) does:

$$\frac{\partial^2 \phi}{\partial t^2} = c^2 \left(\nabla^2 - \frac{m_0^2 c^2}{\hbar^2} \right) \phi \quad (24)$$

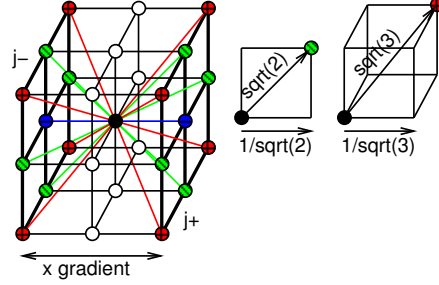


Figure 2: Computation of the spatial gradient using all 18 neighbors that have a non-zero projection along a given axis (in this case, looking at the x axis). The two face points (+, - along the axis) have a full projection along the axis, and thus enter with a weight of 1. The 8 edge points each have a $\frac{1}{\sqrt{2}}$ projection of their overall distance along the axis, and thus contribute with that overall weighting. Similarly, the 8 corners have a $\frac{1}{\sqrt{3}}$ projection weighting. In computing the weighted average, the sum of all neighbor differences is divided by the sum of the weighting terms.

Because differentiation operates independently on the two scalar variables in a complex number, this is equivalent to two parallel scalar KG equations:

$$\frac{\partial^2 \varphi_a}{\partial t^2} = c^2 \left(\nabla^2 - \frac{m_0^2 c^2}{\hbar^2} \right) \varphi_a \quad (25)$$

$$\frac{\partial^2 \varphi_b}{\partial t^2} = c^2 \left(\nabla^2 - \frac{m_0^2 c^2}{\hbar^2} \right) \varphi_b \quad (26)$$

These scalar forms of the complex equations provide the underlying computational mechanisms for the CA model.

The conserved charge value ρ is computed by multiplying the complex KG equation by the complex conjugate:

$$\rho = \frac{i\hbar e}{2m_0 c^2} \left(\phi^* \frac{\partial \phi}{\partial t} - \phi \frac{\partial \phi^*}{\partial t} \right) \quad (27)$$

which reduces to the following locally-computable CA-level equation in terms of the two scalar field components:

$$\rho_i = \frac{\hbar e}{m_0 c^2} (\varphi_{b_i} \dot{\varphi}_{a_i} - \varphi_{a_i} \dot{\varphi}_{b_i}) \quad (28)$$

This equation makes it clear that the charge value represents a coupling across the two otherwise independent variables, which is why a single scalar equation is insufficient.

The current charge density is:

$$\vec{J} = -\frac{i\hbar e}{2m_0} \left(\phi^* \vec{\nabla} \phi - \phi \vec{\nabla} \phi^* \right) \quad (29)$$

which reduces to:

$$\vec{J} = \frac{\hbar e}{m_0 c^2} (\varphi_a \vec{\nabla} \varphi_b - \varphi_b \vec{\nabla} \varphi_a) \quad (30)$$

To compute this in the CA model, we need a discrete approximation of the vector gradient operator $\vec{\nabla} = \left(\frac{\partial}{\partial x}, \frac{\partial}{\partial y}, \frac{\partial}{\partial z} \right)$. This can be derived using the same approach as the 26-neighbor laplacian ([15], Figure 2), using all 18 neighbors (9 vectors) that have a non-zero projection along the axis in question:

$$\frac{\partial s}{\partial x} \approx \frac{1}{\left(2 + \frac{8}{\sqrt{2}} + \frac{8}{\sqrt{3}}\right)} \sum_{j \in \mathcal{N}_9} k_j (\varphi_{j+} - \varphi_{j-}) \quad (31)$$

Where the neighborhood \mathcal{N}_9 contains pairs of points $j+$ and $j-$ that are opposite ends of the 9 rays through the central point, and the distance weighting factors k_j are:

$$\begin{aligned} \text{faces: } k_j &= 1 \\ \text{edges: } k_j &= \frac{1}{\sqrt{2}} \\ \text{corners: } k_j &= \frac{1}{\sqrt{3}} \end{aligned} \quad (32)$$

With these equations, it is now possible for the complex KG equation, implemented in a purely local analog CA model, to produce the charge and current values that serve as sources to Maxwell's equations, completing one half of the coupling. Next, the KG equation must be extended to include coupling with the electromagnetic fields.

B. Minimal Coupling

The electromagnetic field interaction with the electron can be derived through the principle of minimal coupling where the potential enters as an additive term to the first-order derivatives of the system (equivalent to the preservation of local gauge invariance). Because the KG equation is second-order, the equations need to be re-derived using the *gauge covariant derivative* operators (in four-vector notation):

$$\begin{aligned} \partial^\mu &\rightarrow \partial^\mu - \frac{e}{c} A^\mu \\ \partial_\mu &\rightarrow \partial_\mu - \frac{e}{c} A_\mu, \end{aligned} \quad (33)$$

In four-vector notation the basic complex KG equation is:

$$\partial_\mu \partial^\mu \phi = -\frac{m_0^2 c^2}{\hbar^2} \phi,$$

so the minimally-coupled version is:

$$\left(i\hbar \partial_\mu - \frac{e}{c} A_\mu \right)^2 \phi = m_0^2 c^2 \phi. \quad (34)$$

With the spatial and temporal terms separated out, this assumes the form of a standard wave equation:

$$\frac{\partial^2 \phi}{\partial t^2} = c^2 \left(\nabla^2 - \frac{m_0^2 c^2}{\hbar^2} \right) \phi - \frac{2ie}{\hbar} \left(A_0 \frac{\partial \phi}{\partial t} + c \vec{A} \cdot \vec{\nabla} \phi \right) + \frac{e^2 \phi}{\hbar^2} \left(A_0^2 - \vec{A}^2 \right). \quad (35)$$

This is the basic complex KG wave equation, plus some extra terms that involve the interaction between the charge wave and the electromagnetic field potentials A_0 and \vec{A} .

At this point, we have a completely coupled system of charge and electromagnetic fields, all driven fundamentally by the same underlying CA wave equation, plus extra terms. The only thing missing from this picture is *spin*, which is what the Dirac equation adds.

C. Spin and the Second-Order Dirac Equation

The second-order Dirac equation [17, 18] operates on two complex field variables, for a total of four independent degrees of freedom. We denote this field as:

$$\psi = \begin{pmatrix} \varphi_{1a} + i\varphi_{1b} \\ \varphi_{2a} + i\varphi_{2b} \end{pmatrix} \quad (36)$$

The equation is an extension of the complex minimally-coupled KG equation:

$$\left[\left(i\hbar\partial_\mu - \frac{e}{c}A_\mu \right)^2 + \frac{e}{c}\vec{\sigma} \cdot (\vec{B} + i\vec{E}) \right] \psi = m_0^2c^2\psi, \quad (37)$$

where the coupling now involves the electromagnetic vectors \vec{E} and \vec{B} , mediated through the standard Pauli matrices $\vec{\sigma}$ that describe the electron's spin:

$$\vec{\sigma} = \left(\begin{pmatrix} 0 & 1 \\ 1 & 0 \end{pmatrix}, \begin{pmatrix} 0 & -i \\ i & 0 \end{pmatrix}, \begin{pmatrix} 1 & 0 \\ 0 & -1 \end{pmatrix} \right) \quad (38)$$

The resulting CA-style update equations for the second-order derivatives of each of the four charge variables (cell and time indices omitted for simplicity) are:

$$\begin{aligned} \ddot{\varphi}_{1a} = & c^2 \left(\nabla_{26}^2 \varphi_{1a} - \frac{m_0^2 c^2}{\hbar^2} \varphi_{1a} \right) + \frac{2e}{\hbar} \left(A_0 \dot{\varphi}_{1b} + c\vec{A} \cdot \vec{\nabla} \varphi_{1b} \right) + \frac{e^2}{\hbar^2} \varphi_{1a} \left(A_0^2 - \vec{A}^2 \right) + \\ & e \left(\varphi_{1a} B_z - \varphi_{1b} E_z + \varphi_{2a} (B_x + E_y) - \varphi_{2b} (E_x - B_y) \right) \end{aligned} \quad (39)$$

$$\begin{aligned} \ddot{\varphi}_{1b} = & c^2 \left(\nabla_{26}^2 \varphi_{1b} - \frac{m_0^2 c^2}{\hbar^2} \varphi_{1b} \right) - \frac{2e}{\hbar} \left(A_0 \dot{\varphi}_{1a} + c\vec{A} \cdot \vec{\nabla} \varphi_{1a} \right) + \frac{e^2}{\hbar^2} \varphi_{1b} \left(A_0^2 - \vec{A}^2 \right) + \\ & e \left(\varphi_{1b} B_z + \varphi_{1a} E_z + \varphi_{2b} (B_x + E_y) + \varphi_{2a} (E_x - B_y) \right) \end{aligned} \quad (40)$$

$$\begin{aligned} \ddot{\varphi}_{2a} = & c^2 \left(\nabla_{26}^2 \varphi_{2a} - \frac{m_0^2 c^2}{\hbar^2} \varphi_{2a} \right) + \frac{2e}{\hbar} \left(A_0 \dot{\varphi}_{2b} + c\vec{A} \cdot \vec{\nabla} \varphi_{2b} \right) + \frac{e^2}{\hbar^2} \varphi_{2a} \left(A_0^2 - \vec{A}^2 \right) + \\ & e \left(-\varphi_{2a} B_z + \varphi_{2b} E_z + \varphi_{1a} (B_x - E_y) - \varphi_{1b} (E_x + B_y) \right) \end{aligned} \quad (41)$$

$$\begin{aligned} \ddot{\varphi}_{2b} = & c^2 \left(\nabla_{26}^2 \varphi_{2b} - \frac{m_0^2 c^2}{\hbar^2} \varphi_{2b} \right) - \frac{2e}{\hbar} \varphi_{2a} \left(A_0 \dot{\varphi}_{2a} + c\vec{A} \cdot \vec{\nabla} \varphi_{2a} \right) + \frac{e^2}{\hbar^2} \varphi_{2b} \left(A_0^2 - \vec{A}^2 \right) + \\ & e \left(-\varphi_{2b} B_z - \varphi_{2a} E_z + \varphi_{1b} (B_x - E_y) + \varphi_{1a} (E_x + B_y) \right) \end{aligned} \quad (42)$$

Note that the top line of each equation is equivalent to the minimally-coupled complex KG equation, and the second line contains the additional terms that produce spin, as represented in the second-order Dirac equation.

The charge and current equations are somewhat more complex than those for the complex KG equation:

$$\begin{aligned} \rho = & \frac{\hbar e}{m_0 c^2} \left((\varphi_{1b} \dot{\varphi}_{1a} - \varphi_{1a} \dot{\varphi}_{1b}) + (\varphi_{2b} \dot{\varphi}_{2a} - \varphi_{2a} \dot{\varphi}_{2b}) \right) - \\ & \frac{e^2}{m_0 c^2} A_0 (\varphi_{1a}^2 + \varphi_{1b}^2 + \varphi_{2a}^2 + \varphi_{2b}^2) \end{aligned} \quad (43)$$

and:

$$\begin{aligned} \vec{J} = & \frac{\hbar e}{m_0 c^2} \left((\varphi_{1a} \vec{\nabla} \varphi_{1b} - \varphi_{1b} \vec{\nabla} \varphi_{1a}) + (\varphi_{2a} \vec{\nabla} \varphi_{2b} - \varphi_{2b} \vec{\nabla} \varphi_{2a}) \right) - \\ & \frac{e^2}{m_0 c^2} \vec{A} (\varphi_{1a}^2 + \varphi_{1b}^2 + \varphi_{2a}^2 + \varphi_{2b}^2) \end{aligned} \quad (44)$$

At this point we have the full coupled second-order Dirac equation and Maxwell's equations, in the form of local, deterministic continuous-valued CA equations operating on four scalar EM state variables (A_0, \vec{A})

and four scalar Dirac state variables ($\psi = \begin{pmatrix} \varphi_{1a} + i\varphi_{1b} \\ \varphi_{2a} + i\varphi_{2b} \end{pmatrix}$). From these 8 primary state variables, all of the other terms that appear in the equations (e.g., \vec{E} , \vec{B} , ρ , \vec{J}) are computed. Specifically, in the computational implementation, the four Maxwell update equations for A_0 and \vec{A} (equations 14, 15) are computed based on the current values of ρ and \vec{J} , and the second-order Dirac update equations for the Dirac wave field ψ (39 – 42) are computed based on the current values of A_0 and \vec{A} . All of these updated values then become the new current values, and the process repeats. Thus, there is effectively a simultaneous parallel update of all state variables at each point in time.

Although the Dirac equations have become somewhat more complex than the original KG equation, it is important to appreciate that all the constants have a value of 1 in the natural units at the Planck scale, so that makes them somewhat simpler. Furthermore, none of the actual computations involved is more complex than the basic laplacian, and much of it is local to a given cell, so the overall complexity of the system is not high. Arguably, this is the simplest autonomous computational system that can produce the known physics of electrodynamics.

D. Numerical Issues and Symmetry Breaking

If the second-order Dirac update equations (39 – 42) are directly implemented, the system is numerically unstable, even with a fixed electromagnetic field. The source of this instability (which is present even in the simpler coupled complex KG equation), is the coupling between the two elements of the complex variable that occurs in the update equations. Specifically, the update of φ_a depends on φ_b and vice-versa. This interdependency represents a rotation through the φ_a and φ_b variables, driven by the electromagnetic potentials. To the extent that the potentials are pushing the φ_a variable up, there should be an opposite pushing of the φ_b variable down, causing the rotation. However, if the φ_b variable only has the “old” data from the previous time step about how much φ_a got pushed up, then it doesn’t compensate correctly in how much it gets pushed down. This makes the system non-conservative and unstable.

One simple solution to this problem is to break the symmetry between φ_a and φ_b in these update equations. Instead of updating each of them at the same time, based on the prior values of the other, we choose one variable (φ_a , arbitrarily) and update its values first. Then, when we compute φ_b , we use the *current value* of φ_a in the update equation for φ_b . This restores numerical stability to the system.

Interestingly, the need to break the symmetry between these variables fits at least qualitatively with the parity violation associated with the weak force, which is an otherwise surprising and apparently arbitrary aspect of nature. The present imposition of a preferred direction of rotation in these variables, required to make the system numerically stable, could potentially provide a principled motivation for such a symmetry breaking. Further work needs to be done to explore this intriguing possibility.

E. Edges

In finite-sized computational simulations of this system, edges pose a significant problem (it is assumed that the actual system is likely infinite in spatial and temporal extent). Because the Dirac field must remain conservative, the only practical solution is to wrap the edges around on the upper and lower bounds, making a toroidal-shaped system. However, if this is done with the electromagnetic field variables, the potentials constantly increase in magnitude over time because there is no spatial dissipation, which is a critical feature of the EM field that produces its $1/r$ characteristic [25]. Therefore, we use damping Sommerfield boundary conditions at the edges (indexed by e instead of i):

$$\dot{A}_{0e}^{t+1} = c^2 \nabla_{26}^2 A_{0e}^t \quad (45)$$

(i.e., the first derivative is set to the usual second derivative value, producing the damping effect described earlier for the simplest neighborhood averaging CA model). This damping partially simulates the dissipation of the EM field through space that would otherwise occur in an infinitely large system. To more accurately simulate the $1/r$ dissipation, a decay term is used when integrating the potential values (again, only at the edges):

$$A_{0e}^{t+1} = (1 - \gamma)A_{0e}^t + \dot{A}_{0e}^{t+1} \quad (46)$$

where $\gamma = .02$ was empirically derived to more accurately simulate a the $1/r$ dissipation of the EM field that would occur in an infinite CA space.

V. A SIMULATED HYDROGEN ATOM

An important feature of the CA framework is that any physical phenomenon of interest can be simulated directly, just by establishing appropriate initial conditions and then observing the evolution of the wave functions over time. There is no need to establish different analytical frameworks for different problems. The disadvantage is that precise quantitative results can only be obtained through lengthy numerical simulations, and establishing a general pattern of behavior requires multiple simulations under varying conditions. Thus, simulation and analytical approaches are complimentary, and mutually informative. Because the self-coupled system in question here is very difficult to analyze [3–9], the simulation approach is of potential value.

Figure 3 shows the wave state configuration and dynamics of simulated hydrogen atom model. The CA “universe” consisted of $198 \times 200 \times 200$ cells, with $c = .5, m_0 = e = \hbar = 1$. In reality, m_0 for an electron is roughly 4.18×10^{-23} in the natural Planck units of the system, and the diameter of a hydrogen atom is 6.19×10^{24} cells wide. Thus, to fit within the limits of the available computational resources (a 28 node beowulf cluster), the simulated hydrogen atom had to be scaled down by a factor of roughly $1/10^{23}$, and the rest mass scaled up to compensate. This scaling introduces significant differences in behavior relative to what would be expected for the real system, because the wavelengths of the system are only a small multiple of the underlying cell size. One consequence of this is that the laplacian calculation, which propagates waves across all 26 of a cell’s neighbors, will result in a bleeding effect for structures that have significant curvature in multiple dimensions at the grid scale. When the waves span over as many cells as those in the realistically-sized system, the laplacian approximation is essentially perfect, and no such bleeding effects would be evident. Thus, this extremely scaled-down model is likely to be somewhat inaccurate, but it nevertheless demonstrates some interesting behavior. Present-day supercomputers could be used to evaluate the scaling behavior across a couple of orders of magnitude, to produce more accurate results.

The nucleus of this simulated atom was constructed by placing a fixed spherical Gaussian-distributed blob of positive charge in the middle of the system. It is assumed that the strong force keeps this charge distribution relatively localized and stable over time. The four Dirac electron charge field variables were initialized in a pattern based on the state that emerged after a moving electron wave packet with negative charge was captured by this positive nucleus charge. The Dirac charge waves rotate and oscillate around the central nucleus, as shown in Figure 3. See the Appendix for detailed parameters. Although some of the charge waves do escape from the initial configuration, the system remains stable up through at least 20,000 time steps (which took nearly a week of computer time to simulate), in the sense that the same configuration of rotation and oscillation persists. This shows that the system does not exhibit the collapse associated with the classical atomic model. Furthermore, other experiments reveal that the wave dynamics clearly settle into states with integral wavelengths around the circumference of the nucleus, as predicted by quantum mechanics. Movies are available at <http://psych.colorado.edu/~oreilly/real.html>.

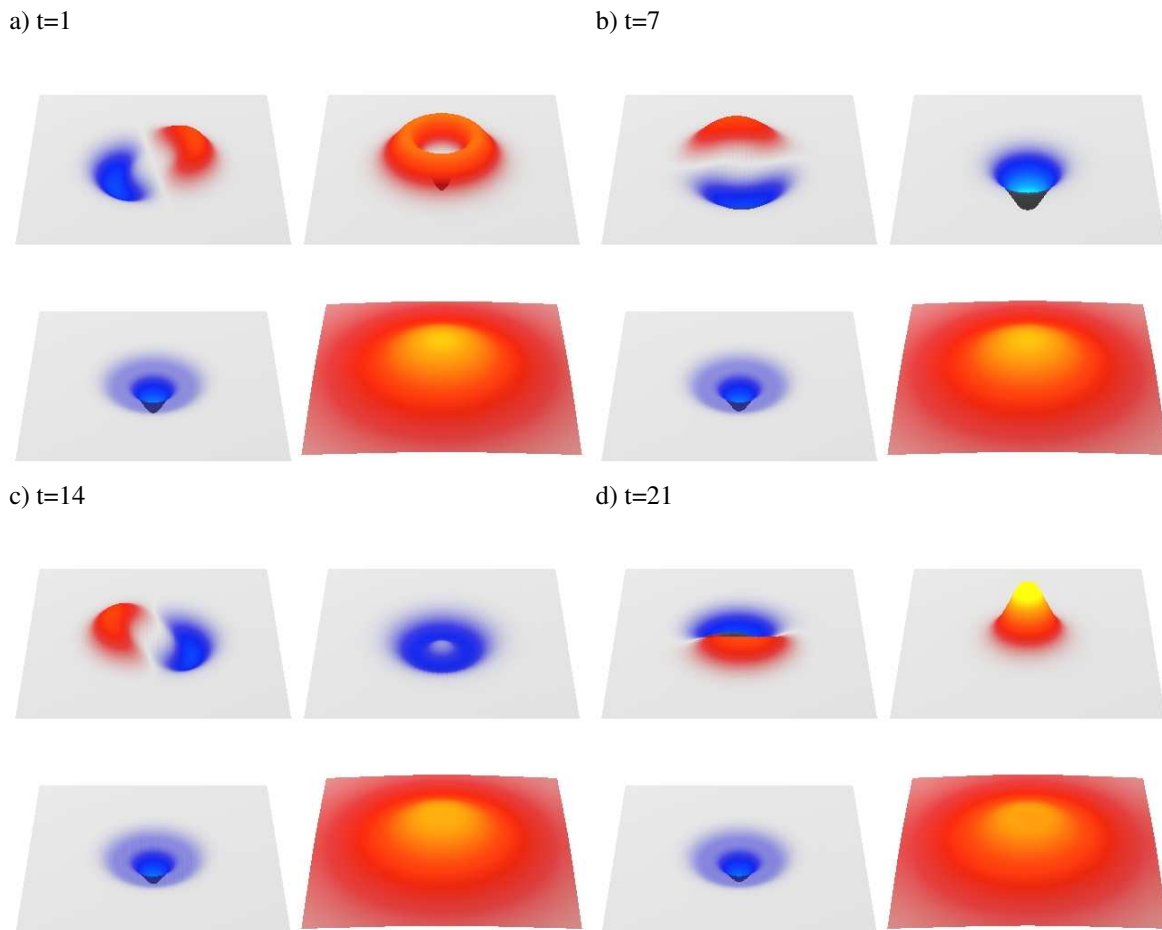


Figure 3: Four time steps from a simulation of a hydrogen atom, produced by placing an electron charge wave around a fixed positive central charge distribution representing the nucleus. For each image, the top-left panel shows the φ_{1a} dirac charge wave field, the top-right is φ_{2a} , bottom-left is the charge density ρ (as generated by the dirac waves only), and bottom-right is the scalar electromagnetic potential A_0 . For each, one slice through a 200^3 sized universe (with edges wrapping around) is plotted, with values coded by height and color (red = positive, blue = negative, zero = transparent grey). The dirac field variables rotate (φ_{1a} , φ_{1b}) and oscillate (φ_{2a} , φ_{2b}) around the central positive charge distribution. The resulting charge ρ is centrally distributed. This pattern remains stable indefinitely, although some of the dirac wave value leaks out over time (but average net charge remains stable, while oscillating over shorter time periods). Movies, and the full simulation software, are available at <http://psych.colorado.edu/~oreilly/real.html>.

Figure 4a shows that the overall charge value of the system is conserved over a longer time frame, but it exhibits a strong oscillatory pattern. Figure 4b shows that the difference between the Lorenz condition and the actual state of the system (the Lorenz error) decreases over time. In both cases, the magnitude of the charge oscillations and the Lorenz error are a function of the frequency of the underlying waves in the system. When a higher frequency atomic configuration was simulated (i.e., a nucleus with a smaller Gaussian width), the Lorenz error was higher, and the charge oscillations were larger in magnitude and higher in frequency. Thus, these effects should be negligible in the system at realistic scales (i.e., roughly 10^{23} times larger).

With respect to the conservation of charge, the following observations can be made. First, if there is no electromagnetic potential at all (or a spatially uniform one), charge is strictly conserved by the Dirac equations at every time step. With a fixed electromagnetic potential that changes over space, charge os-

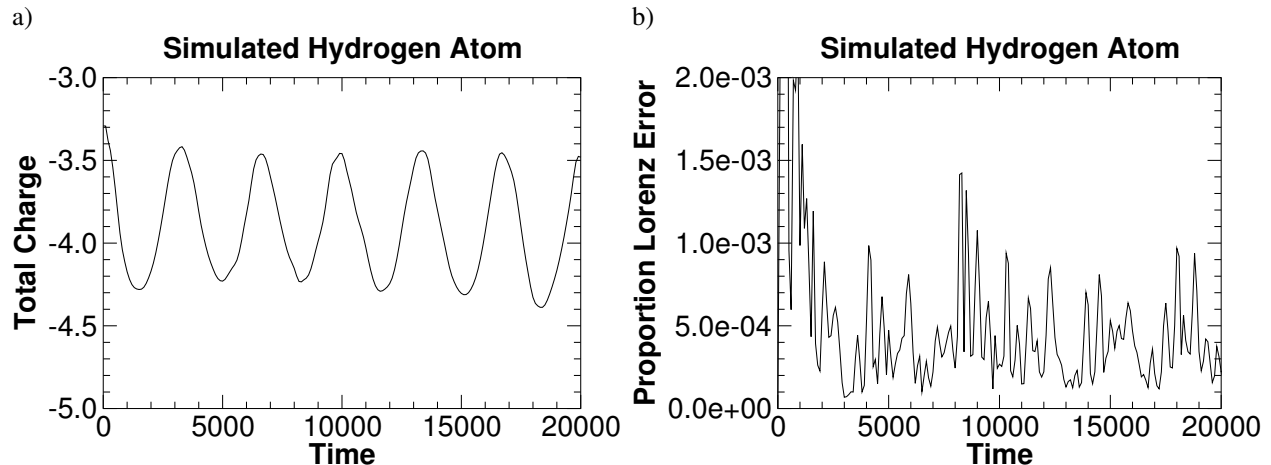


Figure 4: Aggregate behavior of the system over time in the hydrogen atom model. **a)** Total charge in the Dirac electron waves. Although it oscillates, the overall quantity remains roughly constant over time. If the electromagnetic potential is held constant over time, the charge still oscillates, but the long term average is strictly fixed; In the coupled case, precise damping at the edges is required to dissipate the electromagnetic field to maintain constant potential and charge. **b)** Proportion absolute maximum difference (error) between the Lorenz condition ($\frac{\partial A_0}{\partial t} = -c^2 \vec{\nabla} \cdot \vec{A}$) and the actual state of the electromagnetic field.

oscillates as in Figure 4a, but the long time average is strictly conserved. The computed amount of charge depends on where the bulk of the Dirac waves are relative to the spatially-varying potential values, so as Dirac waves move around, the total charge varies, but ultimately the Dirac wave values themselves are fully conserved, so nothing is ever really lost or gained. When the electromagnetic potential is dynamically updated according to Maxwell's equations, it is possible for the overall potential to change over time, resulting in an apparent change in overall charge value over time. Thus, it is important to use the Sommerfeld edge equations with the extra damping term to simulate the $1/r$ dissipation of the field through space, to maintain a constant overall charge value.

VI. DISCUSSION

In summary, this paper shows that a completely coupled Dirac-Maxwell system can be modeled using second-order wave equations (plus additional terms) in an analog cellular automaton, where such second-order wave dynamics emerge from one of the simplest possible update equations that do anything interesting. This system can simulate how the electron wave function behaves in a hydrogen atom: the resulting system appears stable over time, despite being simulated on an extremely small scale where distortions in the laplacian approximation are evident. Sufficiently larger-scale models could be simulated on a modern supercomputer to enable the generation of relatively precise predictions about the behavior of the simulated hydrogen model, which could then be compared with known observations (e.g., the Lamb shift, etc).

The present results may provide some additional motivation, and means, for further explorations of the neoclassical electrodynamic model. However, this model faces a number of important challenges, which we briefly discuss in the remaining subsections.

A. Accounting for Particle-Like Effects

In this model, the electron is purely a wave phenomenon: how can this be reconciled with the particle-like effects that require a wave-particle duality in standard quantum theory? The analog CA framework strongly excludes any kind of point-like particle (e.g., a discrete state variable that is active in only one cell at a time, and propagates to neighboring cells over time). Attempts to develop such a model have clearly shown that all manner of motion asymmetries and other complications (e.g., representing the particle's momentum) arise. In contrast, the pure wave model is very elegant, simple, and appealing, and naturally avoids rotational asymmetries through the use of continuous-values propagating smoothly via second-order dynamics. Therefore, we are strongly motivated to consider ways in which particle-like effects can emerge from within a purely wave-based framework.

One specific challenge is to consider why the electron charge would come in specific discrete units? In our CA model, it is easy to create electron waves with any aggregate amount of charge. The Pauli exclusion principle raises other issues: what distinguishes one electron from another, such that the waves making up one avoid mingling with those of another? These and many other conundrums could potentially be resolved if the electron waves exhibited *emergent localization*. The analysis of Radford [8] shows that the Dirac-Maxwell system exhibits an exponential decay in the Dirac variables, such that they become localized and particle-like. Although this behavior was not observed in the present CA model, this is likely because it requires a larger-scale simulation than was possible at the present time. Another possible mechanism for emergent localization is gravitation — Finster and colleagues [7] have analyzed the Dirac-Maxwell-Einstein system and found localization-like effects. Gravitation can also be included in the present system in a natural way, where the gravitational field propagates as a wave driven by local energy, and it dynamically modulates the coupling constants and rate of wave propagation in the Maxwell and Dirac fields [26]. This model of gravitation is consistent with at least the Schwarzschild metric of general relativity, and it exhibits stable Planck-scale black hole dynamics [26]. Thus, future simulations with gravitation included in the present model will explore this possibility.

Assuming that some form of localization emerges, then the Pauli exclusion effects could simply result from the natural tendency of like charges to repel each other. In other words, once separated and localized, the electric field interactions will naturally maintain such a separation. As to the origin of the precise electric charge: this could be an emergent phenomenon as well (i.e., only a specific amount of charge will produce a stable particle-like distribution). Considerable further simulation work on larger scale models could help address these important questions.

This approach to understanding particle-like effects from within a purely wave-based system is similar in many ways to the decoherence/einselection/existential interpretation of quantum physics [27, 28]. Specifically, when realistic, complex systems are considered, the wave functions experience many forces that cause them to decohere in ways that we measure as particle-like effects. For free particles, the effects of electromagnetic force fields may produce localization-like effects, as described above. For bound particles (e.g., in atoms), the energy state is strongly constrained and is what emerges as the most stable measurable property of the system. In other words, the environment constrains the otherwise free-flowing waves to shape the results of measurements. In reality, there are only the waves, but their emergent dynamics produce particle-like effects.

B. Beyond Electrons

How might this CA model framework account for a wider range of phenomena beyond basic electrodynamics? First, one result from neoclassical theory is that a substantial portion of the electron's measured mass comes from its electromagnetic self-energy (e.g., [6]). Thus, one would expect Dirac waves that do not have charge (which can occur for specific phase relationships among the four state variables) would

have considerably less mass. This may provide an appealing model for the neutrino. Furthermore, the other members of the electron family (muon and tau) could have more energetic electromagnetic dynamics, and thus a larger amount of self-energy, producing their larger observed masses. Thus, there is at least the potential for an elegant way of understanding all of the members of the lepton family. Furthermore, the weak force may emerge naturally from nonlinear interactions in this system, and the parity breaking required for numerical stability could provide an explanation for this otherwise puzzling aspect of nature.

Accounting for the fermions would clearly require introducing a new force field to account for features of the strong force. One intriguing aspect of the strong force is that it naturally produces a strong localization effect (i.e., asymptotic freedom). Therefore, it could be that much of the localization and quantization that we observe can be traced back to the nucleus and the strong force: the discrete charge in the nucleus could serve to discretize and quantize the electron waves that interact with it.

C. Conclusion

As the above discussion makes clear, there are many outstanding questions that need to be addressed in future work. A combination of further analytical and larger-scale numerical simulation work will likely be necessary. Perhaps the most intriguing aspect of this work is that the numerical simulations may simulate the fundamental mechanisms at work in nature itself, given their extremely simple and local nature.

VII. APPENDIX: INITIALIZATION PARAMETERS FOR THE HYDROGEN ATOM MODEL

The actual CA universe was 198x200x200 cells, with the 198 required for uniform splitting of the computation along the x axis among 28 separate nodes in the author's computer cluster. The nucleus charge was a spherical non-normalized Gaussian with $\sigma = 32$:

$$\rho_i = ae^{-\frac{\|i-c\|^2}{\sigma^2}} \quad (47)$$

where $\|i - c\|^2$ indicates the squared Euclidean distance from point $i = (x, y, z)$ to the center point $c = (99, 100, 100)$, and the amplitude a was set so that the total such charge was 4.0 across the entire space. The initial scalar potential A_0 was initialized to the state that this positive charge would create by itself (a Gaussian for a radius of 50 from the center, with a $1/r$ field falling off outside of that). The Dirac charge fields were initialized as follows. The φ_{1a} and φ_{1b} fields were initialized with rotating wave packets constructed as a Gaussian-walled spherical shell:

$$\varphi_{1ai} = ae^{-\frac{\|d_i-r\|^2}{\sigma^2}} \quad (48)$$

(where d is the Euclidean distance from the point $i = (x, y, z)$ to the center ($d = \|i - c\|$), with radius $r = 32$, and width of the shell $\sigma = 16$), times a radial sine wave with one period per revolution. The phases and amplitudes of these variables are:

variable	phase (deg)	amplitude
φ_{1a}	90	.0007
$\dot{\varphi}_{1a}$	0	.00014
φ_{2a}	180	.0007
$\dot{\varphi}_{2a}$	90	.00014

The φ_{2a} and φ_{2b} fields were initialized with an oscillating gaussian bump configuration centered over the nucleus, constructed as a sum of two different gaussian's with different σ and amplitude parameters, generated by fitting to the stable pattern that emerged in earlier simulations.

variable	$\sigma = 28$ amplitude	$\sigma = 20$ amplitude
φ_{1b}	.00175	-.00175
$\dot{\varphi}_{1b}$	0	-.00035
φ_{2b}	0	.00175
$\dot{\varphi}_{2b}$.00035	-.00035

Acknowledgments

Thanks to Iwo Bialynicki-Birula, David Masiello, Erik Deumens, David Meyer, and David Hestenes for helpful comments on this work.

-
- [1] I. Bialynicki-Birula, *Physical Review D* **49**, 6920 (1994).
 - [2] D. A. Meyer, *Journal of Statistical Physics* **85**, 551 (1996).
 - [3] E. T. Jaynes and F. W. Cummings, *Proceedings of the IEEE* **51**, 89 (1963).
 - [4] M. D. Crisp and E. T. Jaynes, *Physical Review* **179**, 1253 (1969).
 - [5] A. O. Barut and J. P. Dowling, *Physical Review A* **41**, 2284 (1990).
 - [6] M. D. Crisp, *Physical Review A* **54**, 87 (1996).
 - [7] F. Finster, J. Smoller, and S.-T. Yau, *Modern Physics Letters A* **14**, 1053 (1999).
 - [8] C. J. Radford, *Journal of Physics A: Mathematical and General* **36**, 5663 (2003).
 - [9] D. Masiello, E. Deumens, and Y. Öhrn, *Physical Review A* **71**, 032108 (2005).
 - [10] S. Ulam, *Proceedings of the International Congress on Mathematics, 1950* **2**, 264 (1952).
 - [11] M. Gardner, *Scientific American* **223**, 120 (1970).
 - [12] K. Zuse, *Calculating Space* (MIT Press, Cambridge, MA, 1970).
 - [13] E. Fredkin, *Physica D* **45**, 254 (1990).
 - [14] S. Wolfram, *Review of Modern Physics* **55**, 601 (1983).
 - [15] R. C. O'Reilly and J. M. Beck (unpublished manuscript), URL <http://psych.colorado.edu/~oreilly/real.html>.
 - [16] J. D. Jackson, *Classical Electrodynamics, 3rd Ed.* (John Wiley & Sons, Hoboken, NJ, 1999).
 - [17] R. P. Feynman and M. Gell-Mann, *Physical Review* **100**, 193 (1958).
 - [18] L. C. Hostler, *Journal of Mathematical Physics* **23**, 1179 (1982).
 - [19] W. Greiner, *Relativistic Quantum Mechanics: Wave Equations, 3rd Ed.* (Springer-Verlag, Berlin, 2000).
 - [20] D. M. Gingrich (2004), URL <http://www.phys.ualberta.ca/~gingrich/phys512/phys512.html>.
 - [21] F. Mandl and G. Shaw, *Quantum Field Theory: Revised Edition* (John Wiley & Sons, Chichester, England, 1984).
 - [22] O. Klein, *Zeitschrift für Physik* **37**, 895 (1926).
 - [23] W. Gordon, *Zeitschrift für Physik* **40**, 117 (1927).
 - [24] H. Kragh, *American Journal of Physics* **52**, 1024 (1984).
 - [25] E. T. Whittaker, *Mathematische Annalen* **57**, 333 (1903).
 - [26] R. C. O'Reilly (unpublished manuscript), URL <http://psych.colorado.edu/~oreilly/real.html>.
 - [27] W. H. Zurek, *Physical Review Letters* **90**, 120404 (2003).
 - [28] M. Schlosshauer, *Reviews of Modern Physics* **76**, 1267 (2004).